We sincerely appreciate your thorough review and constructive comments on our manuscript. Your feedback has provided valuable guidance and will help improve the manuscript's structure and clarity. We have carefully considered each comment. Please find our detailed responses below, with author comments (**AC**) highlighted in blue.

RC1's comments:

This manuscript presents a case study for a modeling framework that combines numerical models and laboratory experiments to predict slope factor-of-safety values under pre- and post-fire conditions for a landscape in Victoria, Australia, burned by the 2016 Wye River-Jamieson Track wildfire. This location experienced shallow landslides in response to rainfall approximately 10 months after the fire was contained. The authors predict factors of safety using a hydrological model that simulates subsurface and overland flow given input rainfall, and they use controlled laboratory burn experiments on similar soils collected outside of the burn area to parameterize certain model values. The results of their modeling experiments demonstrate a widespread increase in slope instability as indicated by factors of safety less than 1 after the fire due to increased soil saturation and diminished soil cohesion that overlaps with the location of observed landslides. The focus of this study and the predictive nature of their methods are of scientific value and would be of interest to the community.

However, this reviewer has multiple concerns that need to be addressed before publication can be recommended. These include model selection in the pre-fire versus post-fire cases, choice of model parameter values, details of the controlled laboratory burn experiments, a need for expanded literature review, and insufficient consideration of uncertainty. Each of these topics is described in greater detail below. If these can be satisfactorily addressed, as well as the line-by-line comments at the end of this comment, then this reviewer could recommend publication to the editor.

1. Model selection: two distinct subcategories of the model are chosen for the pre-fire and post-fire cases, namely the "fine sand" model and the "medium-coarse sand" model. These selections are made on the basis of measured grain size distributions and hydraulic conductivity in the controlled burn laboratory experiment. However, it is unclear the impact that this choice alone has on the modeling results, as different equations are used to calculate the factor of safety in these models (i.e., equation 17 for the post-fire case, and equation 18 in the pre-fire case). The post-fire factor of safety equation depends on the depth to groundwater and the distance from the groundwater level to the slip surface. On the other hand, the pre-fire factor of safety equation depends on the depth of the wetting front from the surface. All else held equal, this reviewer wonders how this difference in physical process representation impacts the modeling results.

   AC: Thank you for your valuable comments. We have provided the following responses to the issues you raised and will revise the manuscript accordingly.

In this study, the fine sand model was applied under pre-fire conditions, whereas the medium-coarse sand model was adopted post-fire. This selection was based on experimental results indicating that soil particle size increased and permeability improved after the fire, thereby shifting the dominant hydrological processes. Laboratory particle-size distribution tests indicated that the pre-fire soil was composed of fine sand, making it appropriate to apply the fine sand model for slope stability analysis (Ozaki et al., 2021; Wakai et al., 2019). This model focuses on the position and downward advancement of the wetting front and is therefore suitable for low-permeability materials. During the initial stage of rainfall, water is retained by capillary forces in the unsaturated zone, and the wetting front gradually progresses downward. The groundwater level responds slowly, and full saturation does not occur until the wetting front reaches the initial groundwater level. Consequently, the fine sand model employs **Eq. (1)** to calculate the factor of safety (F_s), emphasizing the influence of wetting front depth. After the fire, the soil was exposed to high temperatures, and laboratory tests showed an increase in particle size and enhanced permeability. As a result, the soil was classified as coarse sand. In the medium-coarse sand model, under higher-permeability conditions, rainfall supply exceeds capillary retention. When under intense rainfall, water can penetrate the unsaturated zone in a short time, significantly raising the groundwater level (Nguyen et al., 2022). The slope response is therefore governed by groundwater-level rise, and the slip surface can rapidly reach saturation and failure conditions. Accordingly, **Eq. (2)** is used to characterize the reduction in shear strength induced by the rise in groundwater level. Both models are supported by published literature and documented parameter tests, and each has clearly defined applicable material domains (Nguyen et al., 2022; Ozaki et al., 2021; Wakai et al., 2019). Thus, they should not be interchanged.

$$F_s = \frac{\tau_f}{\tau} = \frac{c' + \gamma_{sat} \cdot H \cdot cos^2\theta \cdot tan\varphi'}{\gamma_{sat} \cdot H \cdot sin\theta \cdot cos\theta}, \tag{1}$$

$$F_s = \frac{\tau_f}{\tau} = \frac{c' + [\gamma_t \cdot h_1 + (\gamma_{sat} - \gamma_w) h_2] cos^2\theta \cdot tan\varphi'}{(\gamma_t \cdot h_1 + \gamma_{sat} \cdot h_2) sin\theta \cdot cos\theta}, \tag{2}$$

where τ is the shear stress due to the sliding direction component of gravity of soil; τ_f is the shear strength of soil, which is the maximum shear resistance; γ_t is the wet unit weight of soil; γ_{sat} is the saturated unit weight of soil; γ_w is the unit weight of water; h_1 is the depth from the ground surface to the groundwater level; h_2 is the depth from the groundwater level to the slip surface, which may correspond to the surface of the base layer; H is the depth from the ground surface to the wetting front; θ is the slope inclination angle; c' is the cohesion of soil; and φ' is the angle of shear resistance of soil.

Following your suggestion, we conducted a sensitivity analysis: under the same rainfall and soil parameters, we switched only the F_s calculation formula (fine sand model versus medium-coarse sand model) to compare their effects on the F_s results. Under the pre-fire parameter conditions, F_s values across the study area were calculated using both the fine sand model (the primary model in this study) and the medium-coarse sand model (**Figure R1a** and **Figure R1b**). The results from both models show that $F_s > 1$ across the entire area, with no unstable points. However, the absolute F_s values at the same locations differed significantly between the two models, with an average difference of about 20% and a maximum difference exceeding 50%. This indicates that even when the slope stability assessment results are consistent, the model structure has a substantial influence on the quantitative F_s

values. Furthermore, as shown in **Figure R2**, the F_S results were calculated under post-fire parameter conditions. **Figure R2a** and **Figure R2b** represent the simulation results from the fine sand model and the medium-coarse sand model (the primary model in this study), respectively. It can be observed that the F_S values obtained using the fine sand model are all greater than 1, indicating that the entire area is classified as stable. However, when compared with the zones where landslides were observed, the fine sand model clearly underestimates the actual landslide hazard. In contrast, the medium-coarse sand model identifies multiple points with $F_S < 1$, which correspond well with the locations of the observed landslides.

Based on the above results, under pre-fire parameter conditions, the material properties remain far from the instability threshold. Therefore, all points were classified as stable ($F_S > 1$), regardless of the model structure chosen. However, after the fire, material strength decreased, and only the model that correctly matched the underlying physical mechanisms (the medium-coarse sand model) can identify the actual landslide locations, while the mismatched model (the fine sand model) underestimated the hazard. Therefore, it is difficult to describe the soil changes examined in this study using a single unified formula. In this study, we propose to apply separate models for pre-fire and post-fire conditions precisely to ensure that the physical mechanisms are properly matched.

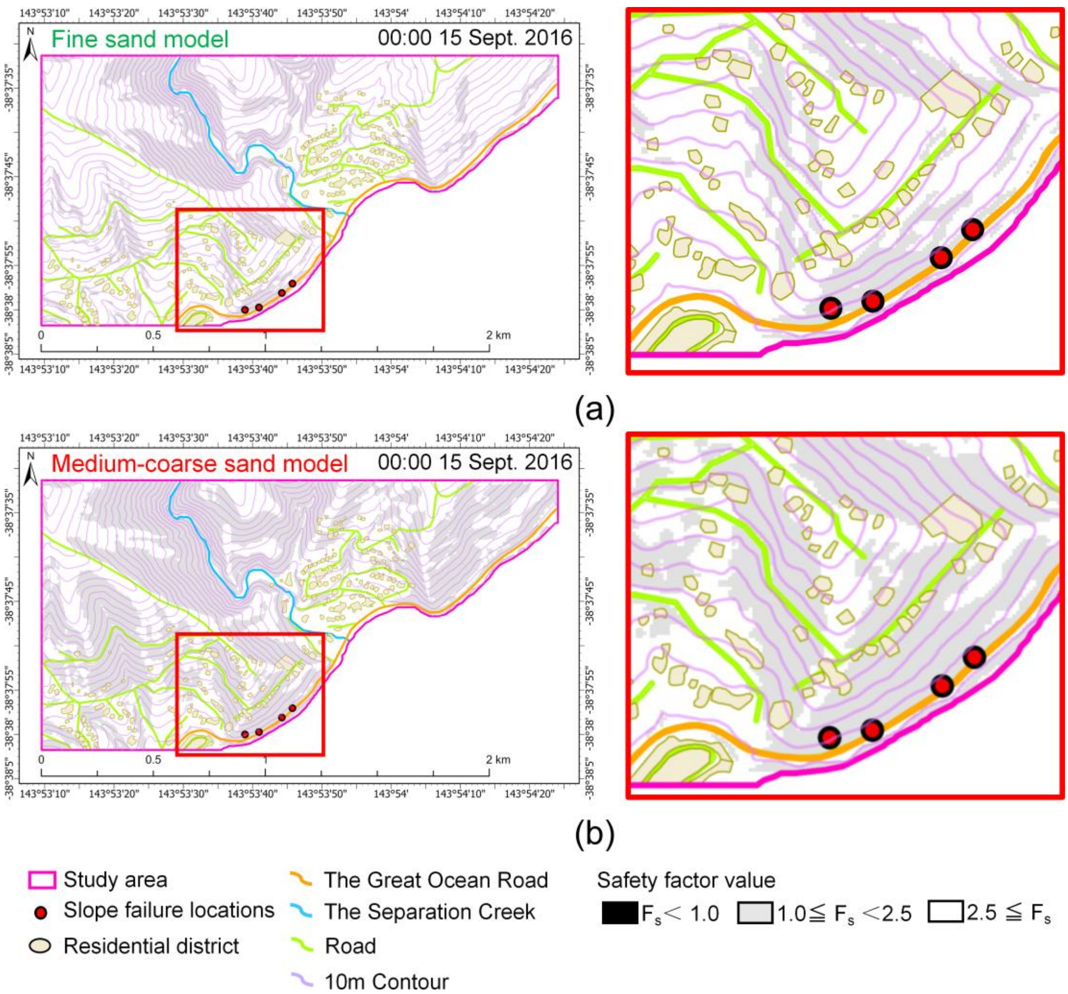

Figure R1: Maps of safety factor under pre-fire conditions: (a) fine sand model and (b) medium-coarse sand model.

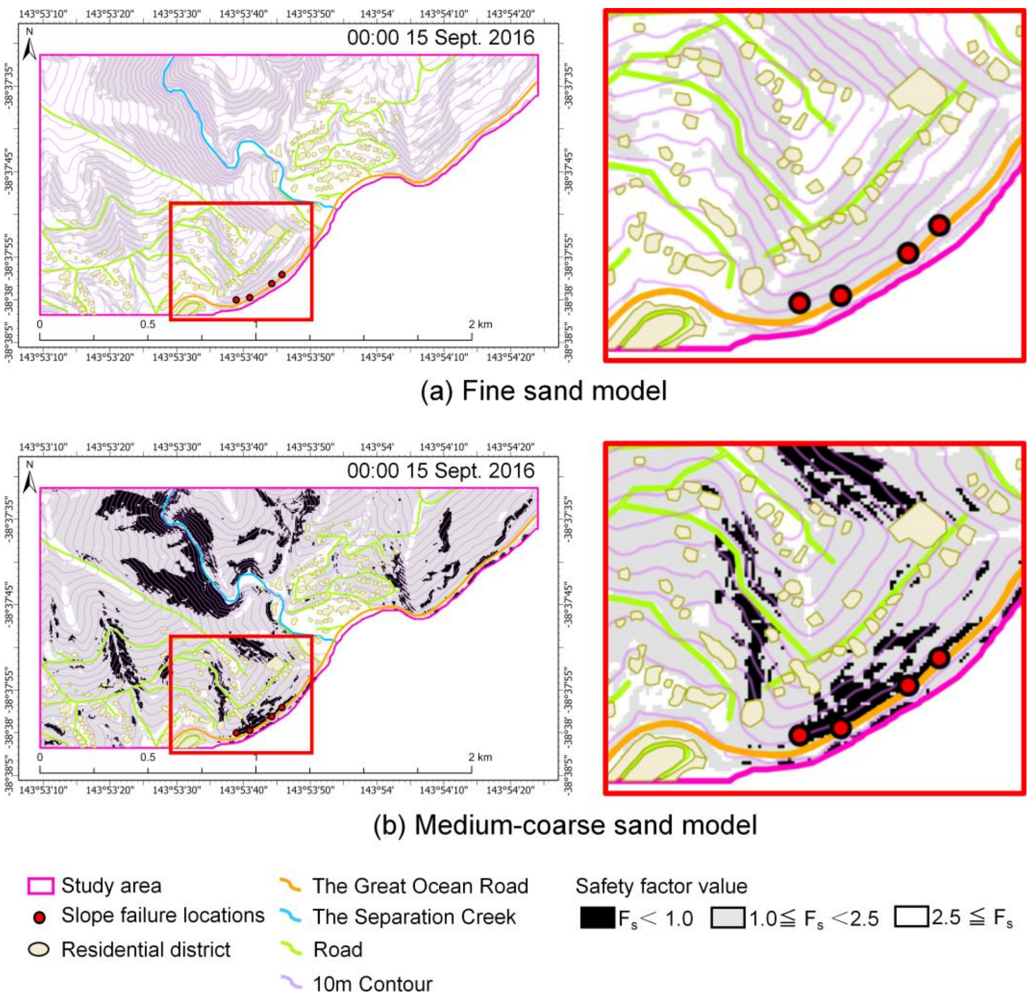

Figure R2: Maps of safety factor under post-fire conditions: (a) fine sand model and (b) medium-coarse sand model.

2. Choice of model parameters: a key choice is made by the authors in determining the depth of soil and the initial position of the groundwater table. Whereas the maximum soil depth is taken to be 2m in the pre-fire case, the maximum soil depth is 0.3m in the post-fire case. This is likely appropriate when considering the depth of mobilizable material as fire modifications to the near-surface soil decrease soil cohesion, as the authors describe on lines 354-357. However, in the hydrological modeling component of the study, the authors state on lines 363-364 that "…the initial groundwater level is assumed to be at the bottom of the soil depth." That is, the initial groundwater level is taken to be 2.0m below the surface in the pre-fire case and 0.3m below the surface in the post-fire case. Considering that the depth to groundwater and the distance between the groundwater level and the potential landslide slip surface are key inputs to the post-fire factor of safety equation, it is unclear what impact this difference in groundwater level assumption has on the study results.

AC: Thank you for your valuable comments. Regarding the specification of soil thickness and initial groundwater level, and their impacts on the simulation results, our responses are as follows. The manuscript will be revised accordingly.

In this study, "soil thickness" is defined as the thickness of the mobilizable shallow soil layer that is susceptible to failure under rainfall in shallow landslides. The spatial distribution of this parameter is based on the inverse relationship between slope angle and soil thickness proposed by Saulnier et al. (1997) (**Eq. 3**), which requires defining the minimum and maximum soil thickness values for the study area. Under the pre-fire case, soil thickness represents the total soil depth from the surface to bedrock, and the maximum thickness (2.0 m) is based on the soil depth map of Australia (Rossel et al., 2014). Under the post-fire case, to more accurately reflect changes in slope physical mechanisms induced by fire, the maximum thickness is not taken as the full depth to bedrock but is determined by two factors: first, fire enhances shallow soil hydrophobicity, creating an impermeable layer above the bedrock; second, root reinforcement is reduced after the fire. Some studies indicated that root concentrations of Eucalyptus are particularly high in the surface 0.3 m of soil and decline sharply with depth (Baldwin and Stewart, 1987; Grant et al., 2012). Thus, after the fire, reinforcement loss at this depth is most significant, making it the most sensitive layer for potential slip surfaces. Therefore, the maximum thickness is set to 0.3 m to reflect the mobilizable soil thickness under the combined influence of root loss and soil hydrophobicity.

$$y_i = y_{max}\left[1 - \frac{tan(x_i) - tan(x_{min})}{tan(x_{max}) - tan(x_{min})}(1-\alpha)\right] , \quad (3)$$

where y_i is the soil depth distribution; $\alpha = y_{min}/y_{max}$; y_{min} and y_{max} are the minimum and maximum values of effective soil depth, respectively; x_i is the slope angle at element i; and x_{max} and x_{min} are the maximum and minimum values of slope angle, respectively.

Regarding the initial groundwater level, the source literature for the models used in this study (Nguyen et al., 2022; Ozaki et al., 2021; Wakai et al., 2019) states that, in the absence of measured groundwater data, the initial groundwater level is generally assumed to lie immediately above the impermeable layer (i.e., at the base of the soil layer or the bedrock interface). This assumption facilitates parameter consistency and model initialization, and has also been widely employed in several representative models in the field of shallow landslide modeling (Baum et al., 2002; Baum et al., 2008; Baum et al., 2010; Iverson, 2000). Because groundwater monitoring data are lacking in the study area, and precipitation recorded at the Lorne (Mount Cowley) rain station during the 24 hours (September 11) preceding the simulation period (September 12–14) totaled only 1 mm (data provided by the Bureau of Meteorology), it is reasonable to assume that the initial groundwater level coincides with the top of the impermeable layer.

We also recognize that the above parameter settings involve certain scientific simplifications and limitations due to spatial variability. In future work, we will incorporate additional field observations and sensitivity analyses to refine the model assumptions.

3. Controlled burn laboratory experiments: the authors used a laboratory furnace to simulate burn conditions using soil samples collected from a nearby unburned area with similar bioclimate and pedogenic characteristics. There are multiple points:

    1. Why were burn experiments conducted at such an extreme temperature (800 °C), and how dependent are the measured soil properties on this temperature? Most controlled laboratory burn experiments go up to ~500-600 °C at the surface, even for the high-severity burn cases (e.g., Doerr et al., 2004; Massman, 2015; Moody et al., 2005; Moody et al., 2009; Wieting et al., 2017); even when surface soil temperatures exceed 800 °C, subsurface temperatures are unlikely to approach this value (Robichaud and Hungerford, 2000).

    2. With regard to the minidisk infiltrometers, did the authors use the equation of Vandervaere et al. (2000) to compute hydraulic conductivity, or a different method? And, were only 5 measurements taken using the minidisk infiltrometer for the unburned soil? The fit of the curve to data in Figure 8a shows considerable scatter, and estimates of hydraulic conductivity from minidisk infiltrometers tend to improve with longer measurement times due to its scaling with $(t^{0.5})^2$.

AC: Thank you for your valuable comment. We have provided a response below and will revise the manuscript accordingly.

We determined 800°C as the maximum temperature for the experiment, mainly referring to relevant studies indicating that the peak temperature at the soil surface could indeed reach or even exceed 800°C under high-intensity wildfire conditions (Soto et al., 1991; Mataix-Solera et al., 2011; Goudie et al., 1992). On the other hand, we also recognize that soils have low heat transfer and temperature decreases rapidly with depth. As you pointed out, this maximum high temperature is primarily confined to the surface layer of soils. Therefore, this maximum temperature setting for this study is focused on simulating the worst-case situation for shallow surface soils on slopes under the influence of high-severity fires. We will make this point clear in the revised manuscript. In addition, we recognize the complexity of profile temperature gradients and soil response at different depths, and consider it as a direction for future research expansion.

In this study, hydraulic conductivity was calculated using the method proposed in the manual of the Mini Disk Infiltrometer (Zhang, 1997). Specifically, cumulative infiltration (I) was plotted against the square root of time ($\sqrt{t}$), and the resulting data were fitted with the following function:

$$I = C_1\sqrt{t} + C_2 t \ , \tag{4}$$

where C_1 (m s^{-1}) and C_2 (m s^{-1}) are parameters. C_1 is related to soil sorptivity, and C_2 is a fitting parameter. The hydraulic conductivity (K) was then computed from:

$$K = C_1/A \ , \tag{5}$$

where A is a value related to the van Genuchten parameters for the soil texture, the suction rate, and the radius of the infiltrometer disk; A values for common soil textures and suctions are provided in the instrument manual (Carsel and Parrish, 1988). The Mini Disk Infiltrometer infiltrates water at a suction of −0.5 to −6 cm and has a radius of 2.25 cm.

In the Mini Disk Infiltrometer test on unburned soil, the suction was set to –2 cm and the experiment was run for 3600 s. Infiltration was recorded every 900 s, yielding five data points and a cumulative infiltration volume of 4 mL (equivalent to 0.25 cm of infiltration). We attempted to extend the test, but because the soil has very low permeability, the infiltration rate remained slow. Therefore, adding further data points was of limited practical value. We found an error in Figure 8a in the original manuscript and will correct it in the revised version (**Figure R3**), but this correction does not affect the input parameters and the main conclusions.

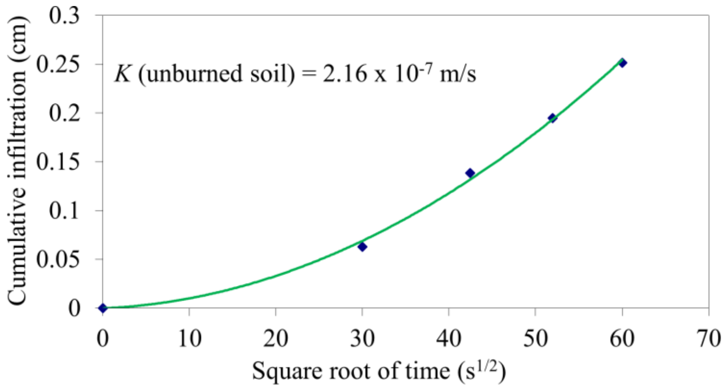

Figure R3: Infiltrometer test results for hydraulic conductivity before burning.

4. Expanded literature review on post-fire infiltration rates: a throughline of the manuscript is that infiltration increases after fire. For instance, the authors state in the first line of the manuscript that “Bushfire… leads to… increased soil infiltration.” As a general statement, this is not true. The response of soil hydraulic properties and infiltration rates to fire is complex (e.g., Shakesby and Doerr, 2006), but it has most commonly been found to substantially decrease after fire due to hydrophobicity effects and return to pre-fire levels over a number of years (e.g., Cerdà, 1998; Ebel, 2019; Ebel et al., 2022; Larson-Nash et al., 2018; Lucas-Borja et al., 2022; Moody et al., 2015; Nyman et al., 2014; Robichaud, 2000; see McGuire et al. (2024) and references therein for a thorough review). The authors allude to this fact towards the end of the manuscript on lines 314-318. This is not to say that infiltration rates can be higher in the first year after fire (e.g., Hoch et al., 2021; Perkins et al., 2022), but the issue is more nuanced than currently stated. The manuscript would be strengthened by a more thorough description of the literature on this topic in the Introduction and would provide the authors a base from which to argue that soil hydrophobicity had diminished at their study site at the time of the landslides, less than 1 year after fire containment, resulting in higher infiltration rates than before the fire. The authors are encouraged to use the citations included here in addition to others they may wish to include.

AC: Thank you for your constructive comments, which have provided valuable guidance for improving our manuscript. Below are our detailed responses and planned revisions.

We agree with the reviewer that our original statement in the first line of the manuscript, "*Bushfire… leads to… increased soil infiltration*" is overly generalized. This wording does not reflect the complexity and temporal variability of post-fire infiltration responses and is therefore not sufficiently accurate. Our initial intention was to emphasize that vegetation loss after a relatively long timescale post-fire may lead to increased infiltration rates. However, such a generalization may cause misunderstanding, and we will correct this statement in the revised manuscript. Additionally, we acknowledge the reviewer's point that many studies reported an initial decrease in soil infiltration after fire due to the development of hydrophobicity in the surface soil layer. In the revised manuscript, we will clarify that post-fire changes in soil infiltration are complex, typically characterized by an initial decrease followed by a potential increase over time as a result of vegetation loss.

We agree with the suggestion that the literature review requires expansion. We have reviewed the references listed by the reviewer and are providing the following brief summary of the content and findings of each study. In the revised introduction, we will add and discuss the references listed by the reviewer above as well as other relevant studies. Based on the expanded literature review, we will clearly present the widely accepted view that post-fire infiltration rates typically show a significant initial decrease followed by gradual recovery over subsequent years. In addition, we will highlight the specific context of our study site, where higher soil infiltration rates were observed approximately 10 months after the fire. To explain this phenomenon, we will include additional supporting references, and provide a more comprehensive discussion of the scenarios and mechanisms that may lead to increased infiltration rates in the short term after fire, thereby supporting the validity of the increased infiltration proposed in this study.

- Cerdà (1998) investigated changes in overland flow and infiltration after a rangeland fire in a Mediterranean scrubland using simulated rainfall experiments. The study found that as vegetation gradually recovered, infiltration rates increased each year, while overland flow decreased from 45% immediately after the fire to less than 6% five and a half years later. Most of the reduction in overland flow occurred within the first two years after the fire.

- Ebel (2019) analyzed 73 sets of plot-scale field-saturated hydraulic conductivity (K_{fs}) data collected within one year after fire and found that K_{fs} decreased significantly, reaching 46% or less of the values observed in unburned plots. No significant differences in K_{fs} were observed between wildfire and prescribed fire, or between moderate and high fire severity. The study also suggested that variations in K_{fs} were more strongly influenced by the measurement method than by spatial scale.

- Ebel et al. (2022) conducted four years of continuous monitoring following the 2013 Black Forest Fire in Colorado, USA, assessing six plots with different initial fire severities. The study analyzed temporal changes in soil-physical and -hydraulic properties—including plot-scale field-saturated hydraulic conductivity (K_{fs}), sorptivity (S), wetting front potential (ψ_f)—as well as surface cover. The results showed that, after the fire, soil bulk density increased and porosity decreased, with these changes being most pronounced in high-severity burn areas. Over time, both soil physical and hydraulic properties showed a trend of recovery, although the recovery was slower in areas with high fire severity.

- Hoch et al. (2021) examined temporal changes in rainfall thresholds for debris flow initiation following wildfire, using three to four years of continuous field and remote sensing observations from three burn areas in the southwestern United States, combined with hydrological modeling. The study found that in the first year after the fire, soil infiltration rates were at their lowest, so even rainfall events with a one-year recurrence interval could trigger debris flows. As soil and vegetation recovered, infiltration capacity increased, and the rainfall threshold for debris flow initiation rose substantially, so that by the third year, rainfall events with recurrence intervals of 10 to 25 years were required to trigger debris flows.

- Larson-Nash et al. (2018) assessed the effects of high-severity fire on small-scale soil infiltration and erosion over five years following the 2003 Hot Creek Fire in Idaho, USA. The results indicated that, due to slow vegetation recovery, the median vegetation cover in burned areas was only 6–8% five years after the fire. Infiltration rates in burned plots consistently remained lower than those in unburned plots, and rill sediment yield remained significantly higher. Relative infiltration rates at shallow depths (1 and 3 cm) showed a moderate to strong correlation with total non-steady infiltration, indicating that shallow soil hydrophobicity was the primary factor limiting infiltration.

- Lucas-Borja et al. (2022) assessed the variability of soil hydraulic conductivity (K) and soil water repellency (SWR) under different fire severities and soil depths in Spanish pine forests and reforested areas. The results indicated that higher fire severity caused more pronounced reductions in surface K and SWR, with maximum decreases of up to 80–90% observed even under low to moderate fire severity. Reforested areas were highly sensitive even to low-severity fires, whereas surface soil water repellency in natural pine forests was less affected.

- McGuire et al. (2024) highlighted that wildfire significantly enhances sediment transport processes by altering soil infiltration capacity, vegetation cover, and sediment availability, with fire severity being a critical factor influencing the trajectories of these geomorphic state variables. Approximately 87% of post-fire debris flow events occur within two years after a wildfire, while landslide-type debris flows tend to occur more than one year after the fire. Changes in geomorphic state following wildfire are most pronounced in the early stages, but may gradually recover to pre-fire conditions within several years or transition to a new steady state, demonstrating diverse recovery pathways.

- Moody et al. (2015) investigated the effects of burn severity on soil hydraulic properties by measuring field-saturated hydraulic conductivity (K_{fs}) and sorptivity (S) of soil samples from the Black Forest Fire area in Colorado, USA, using a laboratory tension infiltrometer under different levels of burn severity, as indicated by the differenced normalized burn ratio (dNBR). The results showed that soil hydraulic properties (K_{fs} and S) declined significantly under high burn severity (dNBR > 420), and the study was the first to establish a quantitative relationship between these properties and burn severity, providing a basis for post-fire hydrological prediction.

- Nyman et al. (2014) quantitatively evaluated the effects of surface storage (H), macropore hydraulic conductivity (K_{mac}), and matrix hydraulic conductivity (K_{mat}) on soil infiltration in three fire-affected areas in southeastern Australia following the 2009 Black Saturday wildfires. A simplified two-layer infiltration model was used in combination with laboratory tension infiltrometer experiments on soil samples. The results showed that the wildfire increased surface soil water repellency, resulting in initial suppression of infiltration, followed by gradual recovery of macropore flow and matrix hydraulic conductivity.

- Perkins et al. (2022) investigated the multi-stage recovery of soil hydraulic properties following the 2017 Nuns and Tubbs wildfires in Northern California. Forty-one monitoring sites were established in grassland, shrubland, and forest areas, where field-saturated hydraulic conductivity (K_{fs}) was repeatedly measured using a tension disc infiltrometer over a 3.5-year period. The study found that K_{fs} declined significantly after the fire, but partially and rapidly recovered after the first rainy season, exhibiting a complex, seasonal, multi-stage recovery process.

- Robichaud (2000) investigated the effects of prescribed fire on soil infiltration rates in Northern Rocky Mountain forests, USA. Simulated rainfall experiments were conducted in unburned, low-severity, and high-severity burn areas across different forest types to measure infiltration rates. The results showed that runoff rates increased significantly at the onset of rainfall in high-severity burn areas, surface soil water repellency was enhanced, and infiltration rates temporarily decreased by 10% to 40%. Infiltration rates in unburned and low-severity burn areas showed little change.

- Shakesby and Doerr (2006) systematically reviewed the effects of wildfire on soil hydraulic properties and infiltration rates, highlighting the complexity of these responses influenced by fire severity, soil type, and environmental conditions, with significant regional variations. Furthermore, the long-term and large-scale impacts of wildfire on hydrological and geomorphological processes remain to be thoroughly investigated. This reference is also cited in Lines 26–27 of the original manuscript: "*Bushfires not only cause immediate losses but also lead to lasting hydrological and geomorphological changes, affecting soil physicochemical properties for months to years (Shakesby and Doerr, 2006).*"

5. Uncertainty of the results: as alluded to in points 1 & 2, the study currently does not consider the uncertainty involved with model selection and parameter choices. This makes it difficult for this reviewer to place confidence in the general predictive ability of the method. The manuscript would benefit from one of a sensitivity analysis of models and model parameters, incorporation of uncertainty through e.g., a Monte Carlo sampling strategy, or inclusion of additional observations in order to separate the data into calibration and validation datasets. However, this reviewer acknowledges that this may difficult or not possible to accomplish due to the limited availability of target data.

AC: Thank you for your valuable suggestions. We agree with the reviewer that the modeling and parameter uncertainty analyses will contribute to the persuasiveness of the study. However, due to the limited observed data and research conditions, we are currently having difficulties in conducting the suggested analyses above. We will explain these limitations in the revised manuscript and consider them as a direction for future research.

Lines 104-106: how deep-seated were these landslides?

AC: Thank you for your valuable comment. Currently, explicit information regarding the depth of the Paddy's Path landslide is not available. Based on the field photographs (**Figure R4**), it is inferred to be a shallow landslide. We will include this clarification in the revised manuscript.

Figure R4: The Paddy's Path landslide observed along the Great Ocean Road during the rainfall period (Colac Herald, 2016; Colls and Miner, 2021).

Line 111: please zoom out on the context map in Figure 1a, readers unfamiliar with Australia will be unable to discern the location of the study area within the continent

AC: Thank you for this helpful suggestion. We have revised **Figure 1** to better show the location of the study area within the Australian continent, as shown below.

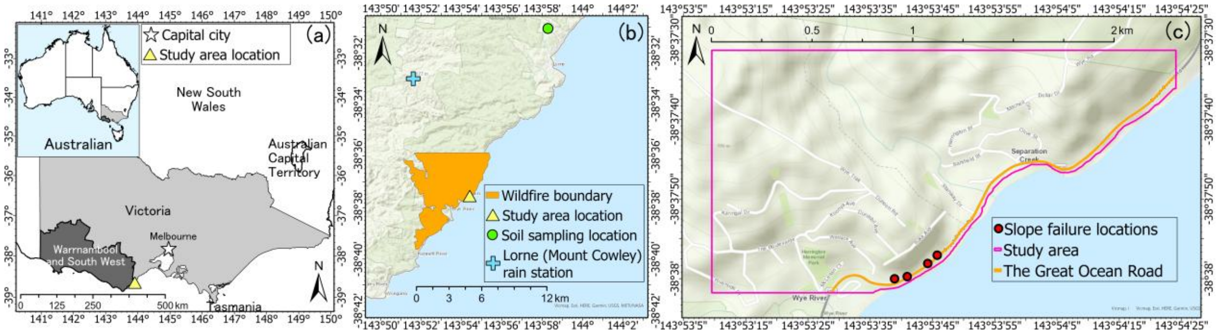

Figure 1: (a) Location of the study area (created using ArcGIS; data from the Australian Bureau of Statistics). (b) Spatial relationship among the wildfire-affected boundary, study area, and soil sampling locations (adapted from Colls and Miner, 2021). (c) Extent of the study area and slope failure locations (created using ArcGIS; data from ESRI).

Lines 137-139: Can the burn severity map be added as an overlay to Figure 1? This would help the reader to understand the burn severity within the study area. This sentence would likely fit better in Section 2.

AC: Thank you for your valuable comments. We agree that adding a burn severity map as an overlay in Figure 1 will enhance the understanding of readers. However, on-site measurements of soil burn severity and sufficiently high-resolution dNBR products are currently difficult to obtain. Therefore, we are unable to provide a burn severity map in the figure. We appreciate your understanding and constructive suggestions. Additionally, we will move the relevant sentence to Section 2 in the revised manuscript.

Line 177: please include how more information about the infiltrometer measurements (e.g., the suction head used, the duration of time/volume that measurements were taken for) and what equations were used to calculate hydraulic conductivity.

AC: Thank you for your valuable comments. We have provided a response below and will revise the manuscript accordingly. In this study, hydraulic conductivity was calculated using the method proposed in the manual of the Mini Disk Infiltrometer (Zhang, 1997). For further details, please read the response to the general comment 3 regarding hydraulic conductivity measurement (p. 6 of this document). The measurement details are as follows: For the unburned soil, a suction head of −2 cm was used, with a total measurement duration of 3600 s, and infiltration was recorded every 900 s, resulting in five data points and a total cumulative infiltration of 4 mL (equivalent to 0.25 cm of infiltration). For the burned soil, a suction head of −1 cm was used, with a total duration of 540 s, infiltration recorded every 60 s, resulting in ten data points and a total infiltration of 30.8 mL (equivalent to 1.94 cm of infiltration). In both cases, the measurement was continued until the infiltration rate reached a steady state.

Line 189: please include the equation(s) used to fit c and φ to the data

AC: Thank you for your helpful suggestion. In this study, we used the Mohr-Coulomb failure criterion ($\tau = c + \sigma \tan \varphi$) to determine the cohesion (c) and internal friction angle (φ), where τ is the shear strength and σ is the normal stress. Specifically, for the unburned soil, the fitted equation is $\tau = 0.8193\,\sigma + 6.4119$; for the burned soil, the fitted equation is $\tau = 0.8463\,\sigma + 0.4462$. The fitted values were rounded to two decimal places. We will include these equations in the revised manuscript to improve clarity.

Line 223: by "lateral infiltration of groundwater", do the authors mean lateral motion?

AC: Thank you for your insightful comment. The term "lateral infiltration of groundwater" refers to the lateral movement of groundwater within the saturated zone of the slope. To avoid any ambiguity, we will revise "lateral infiltration" to "lateral seepage flow" in the manuscript.

Line 266: relating to general comment 1 above, why is the horizontal component of groundwater motion not accounted for in the pre-fire case?

AC: Thank you for your important comment. In the pre-fire case, we adopted a fine sand model that considers only the vertical infiltration of rainwater. According to the source literature of this model (Ozaki et al., 2021), both FEM numerical analysis and parametric studies demonstrated that, for slopes composed of fine-grained, low-permeability soils, rainwater infiltration is predominantly vertical. Thus, water movement can be reasonably represented using a one-dimensional vertical seepage model, and the horizontal component can be justifiably neglected. Only in the case involving coarser-grained soils with higher permeability, or where the slope is particularly steep or has complex subsurface structures, is it necessary to include horizontal flow in the analysis. We will provide further clarification regarding the neglect of the horizontal component in the revised manuscript.

Lines 294-364: Sections 4.5, 5.1, and 5.2 seem to be closely related to each other; the authors may disagree, but they could be placed together in their own separate section

AC: Thank you for your helpful suggestion. We agree with your idea and plan to combine Sections 4.5, 5.1, and 5.2 into a separate section in the revised manuscript.

Line 371: Figure 12 is not referenced in the text

AC: Thank you for pointing this out. We accept this criticism and will reference Figure 12 in the revised manuscript to ensure it is clearly linked to the text.

Line 372: how were the initial saturation degrees determined? Please provide details in the text on why they are different for each case

AC: Thank you for your valuable comment. Below, we has provided an explanation of how the initial degree of saturation was determined. Based on this explanation, we will include a more detailed description in the revised manuscript regarding how the initial saturation degrees and the related parameters were determined.

Given the difficulty in directly obtaining the initial saturation degree (S_{r0}), S_{r0} was calculated using the following equation proposed by Lambe and Whitman (1969), based on laboratory test results for water content (w), soil particle density (ρ_s), and void ratio (e). And ρ_w is the density of water.

$$S_r = \frac{w\rho_s}{e\rho_w} \quad , \tag{6}$$

The difference in S_{r0} between the pre-burned and post-burned conditions mainly results from experimentally determined differences in water content, soil particle density, and void ratio. Below, we have provided an explanation of how these parameters w, ρ_s, and e in the S_{r0} calculation formula were determined.

1) Moisture content, w (%)

- **Unburned:** Undisturbed soil samples consisted of four cylinder samples A; the mean of four measurements was used (see **Figure R5** below).
- **Burned:** The water content for the burned case was referenced from the unburned condition.

2) Soil particle density, ρ_s (g cm⁻³)

- **Unburned:** Disturbed soil samples were tested using three specimens; the mean of their results was used (see **Figure R6a** below).
- **Burned:** Disturbed soil samples after burning were tested using the same procedures as the unburned samples (see **Figure R6b** below).

3) Void ratio, e

- **Unburned:** The value was calculated based on the measured ρ_s, ρ_t and w, using **Eq. (7)** shown below (Lambe and Whitman, 1969).

$$e = \frac{\rho_s\,(1+w)}{\rho_t} - 1 \ , \qquad (7)$$

- **Burned:** For simplicity, the moisture content of burned soil samples was assumed to be zero; the same calculation method as for unburned samples was applied.

4) Wet density, ρ_t (g cm⁻³)

- **Unburned:** Undisturbed soil samples consisted of four cylinder samples A; the mean of four measurements was used (see **Figure R5a** below).
- **Burned:** Considering the practical difficulties of direct measurement, the dry density measured in the laboratory was adopted (see **Figure R7** below).

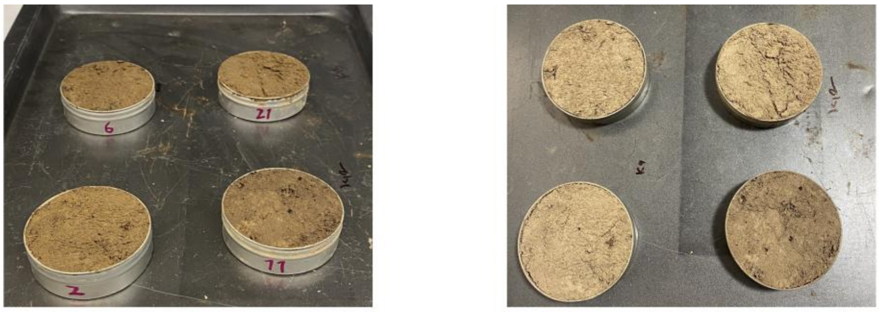

(a) Wet undisturbed cylinder samples A (b) Undisturbed cylinder samples A after being dried

Figure R5: Cylinder samples A for measuring pre-burn water content and wet density.

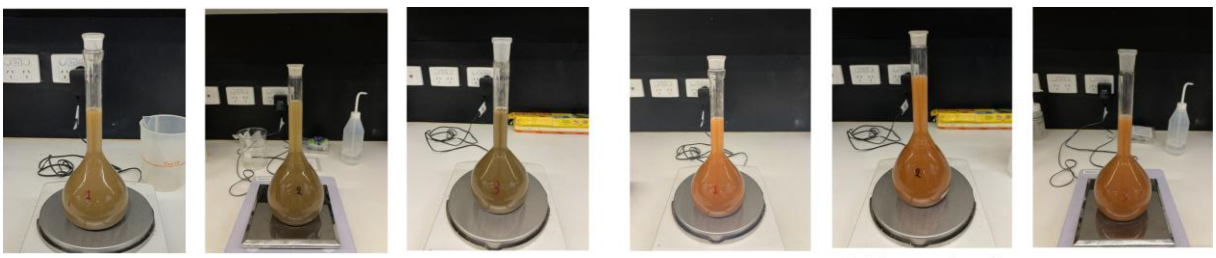

(a) unburned soil (b) burned soil

Figure R6: Soil particle density tests of unburned soil (a) and burned soil (b).

Figure R7: Undisturbed cylinder samples B for measuring post-burning dry density.

Line 373: Please move the Results and Discussion from Section 5.3 to a stand-alone section, e.g. Section 6

AC: Thank you for your constructive suggestion. We will move the Results and Discussion to a new stand-alone section in the revised manuscript.

References

Baldwin, P. J. and Stewart, H. T. L.: Distribution, length and weight of roots in young plantations of Eucalyptus grandis W. Hill ex Maiden irrigated with recycled water, Plant Soil, 97, 243–252, https://doi.org/10.1007/BF02374947, 1987.

Baum, R. L., Godt, J. W., and Savage, W. Z.: Estimating the timing and location of shallow rainfall-induced landslides using a model for transient, unsaturated infiltration, J. Geophys. Res.-Earth Surf., 115, F3, https://doi.org/10.1029/2009JF001321, 2010.

Baum, R. L., Savage, W. Z., and Godt, J. W.: TRIGRS; a Fortran program for transient rainfall infiltration and grid-based regional slope-stability analysis, U.S. Geol. Surv. Open File Rep., 2002–424, https://doi.org/10.3133/ofr02424, 2002.

Baum, R. L., Savage, W. Z., and Godt, J. W.: TRIGRS—A Fortran program for transient rainfall infiltration and grid-based regional slope-stability analysis, version 2.0, U.S. Geol. Surv. Open File Rep., 2008-1159, 75 pp., 2008.

Carsel, R. F. and Parrish, R. S.: Developing joint probability distributions of soil water retention characteristics, Water Resour. Res., 24, 755–769, https://doi.org/10.1029/WR024i005p00755, 1988.

Cerdà, A.: Changes in overland flow and infiltration after a rangeland fire in a Mediterranean scrubland, Hydrol. Process., 12, 1031–1042, 1998.

Colac Herald: Ocean Road towns on landslide watch, https://colacherald.com.au/2016/09/ocean-road-towns-landslide-watch/, last access: 28 May 2025, 2016.

Colls, S. and Miner, A. S.: Bushfires, landslides and geotechnical challenges in the Otway Ranges, Victoria, in: NZGS Symposium 2021, Dunedin, New Zealand, 24–26 March 2021, 2021.

Doerr, S. H., Blake, W. H., Shakesby, R. A., Stagnitti, F., Vuurens, S. H., Humphreys, G. S., and Wallbrink, P.: Heating effects on water repellency in Australian eucalypt forest soils and their value in estimating wildfire soil temperatures, Int. J. Wildland Fire, 13, 157–163, https://doi.org/10.1071/WF03051, 2004.

Ebel, B. A., Moody, J. A., and Martin, D. A.: Post-fire temporal trends in soil-physical and -hydraulic properties and simulated runoff generation: Insights from different burn severities in the 2013 Black Forest Fire, CO, USA, Sci. Total Environ., 802, 149847, https://doi.org/10.1016/j.scitotenv.2021.149847, 2022.

Ebel, B. A.: Measurement method has a larger impact than spatial scale for plot-scale field-saturated hydraulic conductivity (Kfs) after wildfire and prescribed fire in forests, Earth Surf. Process. Landf., 44, 1945–1956, https://doi.org/10.1002/esp.4621, 2019.

Goudie, A. S., Allison, R. J., and McLaren, S. J.: The relations between modulus of elasticity and temperature in the context of the experimental simulation of rock weathering by fire, Earth Surf. Process. Landf., 17, 605–615, https://doi.org/10.1002/esp.3290170606, 1992.

Grant, J. C., Nichols, J. D., Yao, R. L., Smith, R. G. B., Brennan, P. D., and Vanclay, J. K.: Depth distribution of roots of Eucalyptus dunnii and Corymbia citriodora subsp. Variegata in different soil conditions, For. Ecol. Manage., 269, 249–258, https://doi.org/10.1016/j.foreco.2011.12.033, 2012.

Hoch, O. J., McGuire, L. A., Youberg, A. M., and Rengers, F. K.: Hydrogeomorphic recovery and temporal changes in rainfall thresholds for debris flows following wildfire, J. Geophys. Res.-Earth Surf., 126, e2021JF006374, https://doi.org/10.1029/2021JF006374, 2021.

Iverson, R. M.: Landslide triggering by rain infiltration, Water Resour. Res., 36, 1897–1910, https://doi.org/10.1029/2000WR900090, 2000.

Lambe, T. W. and Whitman, R. V.: Soil Mechanics, John Wiley & Sons, New York, 553 pp., ISBN 9780471511922, 1969.

Larson-Nash, S. S., Martin, D. A., Johansen, M. P., Wagenbrenner, J. W., and MacDonald, L. H.: Recovery of small-scale infiltration and erosion after wildfires, J. Hydrol. Hydromech., 66, 261–270, https://doi.org/10.1515/johh-2017-0056, 2018.

Lucas-Borja, M. E., Fernández, C., Plaza-Alvarez, P. A., and Zema, D. A.: Variability of hydraulic conductivity and water repellency of soils with fire severity in pine forests and reforested areas under Mediterranean conditions, Ecohydrology, 15, e2472, https://doi.org/10.1002/eco.2472, 2022.

Massman, W. J.: A non-equilibrium model for soil heating and moisture transport during extreme surface heating: the soil (heat–moisture–vapor) HMV-Model Version 1, Geosci. Model Dev., 8, 3659–3680, https://doi.org/10.5194/gmd-8-3659-2015, 2015.

Mataix-Solera, J., Cerdà, A., Arcenegui, V., Jordán, A., and Zavala, L. M.: Fire effects on soil aggregation: A review, Earth-Sci. Rev., 109, 44–60, https://doi.org/10.1016/j.earscirev.2011.08.002, 2011.

McGuire, L. A., Ebel, B. A., Rengers, F. K., Kean, J. W., and Smith, J. D.: Fire effects on geomorphic processes, Nat. Rev. Earth Environ., 5, 486–503, https://doi.org/10.1038/s43017-024-00557-7, 2024.

Moody, J. A., Ebel, B. A., Nyman, P., Martin, D. A., Stoof, C., and McKinley, R.: Relations between soil hydraulic properties and burn severity, Int. J. Wildland Fire, 25, 279–293, https://doi.org/10.1071/WF14062, 2015.

Moody, J. A., Kinner, D. A., and Úbeda, X.: Linking hydraulic properties of fire-affected soils to infiltration and water repellency, J. Hydrol., 379, 291–303, https://doi.org/10.1016/j.jhydrol.2009.10.015, 2009.

Moody, J. A., Smith, J. D., and Ragan, B. W.: Critical shear stress for erosion of cohesive soils subjected to temperatures typical of wildfires, J. Geophys. Res., 110, F01004, https://doi.org/10.1029/2004JF000141, 2005.

Nguyen, V. T., Wakai, A., Sato, G., Viet, T. T., and Kitamura, N.: Simple method for shallow landslide prediction based on wide-area terrain analysis incorporated with surface and subsurface flows, Nat. Hazards Rev., 23, 04022028, https://doi.org/10.1061/(ASCE)NH.1527-6996.0000578, 2022.

Nyman, P., Sheridan, G. J., Smith, H. G., and Lane, P. N.: Modeling the effects of surface storage, macropore flow and water repellency on infiltration after wildfire, J. Hydrol., 513, 301–313, https://doi.org/10.1016/j.jhydrol.2014.02.044, 2014.

Ozaki, T., Wakai, A., Watanabe, A., Cai, F., Sato, G., and Kimura, T.: A simplified model for the infiltration of rainwater in natural slope consisting of fine sands, Jpn. Landslide Soc. J., 58, 57–64, https://doi.org/10.3313/jls.58.57, 2021.

Perkins, J. P., Diaz, C., Corbett, S. C., Cerovski-Darriau, C., Stock, J. D., Prancevic, J. P., et al.: Multi-stage soil-hydraulic recovery and limited ravel accumulations following the 2017 Nuns and Tubbs wildfires in Northern California, J. Geophys. Res.-Earth Surf., 127, e2022JF006591, https://doi.org/10.1029/2022JF006591, 2022.

Robichaud, P. R. and Hungerford, R. D.: Water repellency by laboratory burning of four northern Rocky Mountain forest soils, J. Hydrol., 231, 207–219, https://doi.org/10.1016/S0022-1694(00)00195-5, 2000.

Robichaud, P. R.: Fire effects on infiltration rates after prescribed fire in Northern Rocky Mountain forests, USA, J. Hydrol., 231–232, 220–229, https://doi.org/10.1016/S0022-1694(00)00196-7, 2000.

Rossel, R. A. V., Chen, C., Grundy, M., Searle, R., Clifford, D., Odgers, N., Holmes, K., and Kidd, D.: Clay (3″ resolution) − Soil and Landscape Grid National Soil Attribute Maps, CSIRO [data set], https://doi.org/10.4225/08/546EEE35164BF, 2014.

Saulnier, G.-M., Beven, K., and Obled, C.: Including spatially variable effective soil depths in TOPMODEL, J. Hydrol., 202, 158–172, https://doi.org/10.1016/S0022-1694(97)00059-0, 1997.

Shakesby, R. A. and Doerr, S. H.: Wildfire as a hydrological and geomorphological agent, Earth-Sci. Rev., 74, 269–307, https://doi.org/10.1016/j.earscirev.2005.10.006, 2006.

Soto, B., Benito, E., and Diaz-Fierros, F.: Heat-induced degradation processes in forest soils, Int. J. Wildland Fire, 1, 147–152, https://doi.org/10.1071/wf9910147, 1991.

Vandervaere, J., Vauclin, M., and Elrick, D. E.: Transient flow from tension infiltrometers I. The two-parameter equation, Soil Sci. Soc. Am. J., 64, 1263–1272, https://doi.org/10.2136/sssaj2000.6441263x, 2000.

Wakai, A., Hori, K., Watanabe, A., Cai, F., Fukazu, H., Goto, S., and Kimura, T.: A simple prediction model for shallow groundwater level rise in natural slopes based on finite element solutions, Jpn. Landslide Soc. J., 56, 227–239, https://doi.org/10.3313/jls.56.227, 2019.

Wieting, C., Ebel, B. A., and Singha, K.: Quantifying the effects of wildfire on changes in soil properties by surface burning of soils from the Boulder Creek Critical Zone Observatory, J. Hydrol.: Reg. Stud., 13, 43–57, https://doi.org/10.1016/j.ejrh.2017.07.006, 2017.

Zhang, R.: Determination of soil sorptivity and hydraulic conductivity from the disk infiltrometer, Soil Sci. Soc. Am. J., 61, 1024–1030, https://doi.org/10.2136/sssaj1997.03615995006100040005x, 1997.